The Behavior of Thiacarbocyanine Dyes on the Surface of Few-Layered Hexagonal Boron Nitride

AUTHORS

Anne-Charlotte Nellissen[a], Roelof Steeno[a], Jonathan B.F. Vandenwijngaerden[a], Steven De Feyter[a], Stijn F.L. Mertens[b,*] & Mark Van der Auweraer[a,*]

AFFILIATIONS

[a]Laboratory for Photochemistry and Spectroscopy, KU Leuven (Chem & Tech, Celestijnenlaan 200F, 3001 Leuven, Belgium)

[b]Department of Chemistry, Energy Lancaster and Materials Science Institute, Lancaster University (Bailrigg, LA1 4YB Lancaster, United Kingdom)

*Corresponding authors: s.mertens@lancaster.ac.uk or stmerten@gmail.com & mark.vanderauweraer@kuleuven.be

KEYWORDS

Thiacarbocyanine dyes, hexagonal boron nitride, dye self-assembly and steady-state spectroscopy

ABSTRACT

The adsorption and self-assembly of several thiacarbocyanine dyes on hexagonal boron nitride (hBN) was investigated by combining steady-state spectroscopy and atomic force microscopy. The adsorption isotherms indicate that at saturation the density of the cationic TDC (5,5-dichloro-3-3'-diethyl-9-ethyl-thiacarbocyanine) molecules on hBN is similar to that of TD2 (3-3'-diethyl-9-ethyl-thiacarbocyanine) molecules, while the densities of TD0 (3-3'-diethyl-thiacarbocyanine) molecules and the zwitterionic THIATS (5,5-dichloro-3-3'-disulfopropyl-9-ethyl-thiacarbocyanine) molecules are significantly higher. The intermolecular distances between neighboring adsorbed dyes, calculated from these saturation densities indicate a flat-

on adsorption for TDC, TD2 and TD0 and a partial edge-on adsorption for THIATS. AFM micrographs of the adsorbed TDC, TD0 and THIATS molecules indicate that already at low dye concentrations in the solution, where only a small fraction of the hBN surface is covered, the dye molecules already form upon adsorption to hBN aggregates of at least 10 nm, separated by areas where no adsorbed dye molecules can be detected. The resolution of the micrographs was however insufficient to show details of the packing of the adsorbed molecules. For THIATS, the thickness of the adsorbed layer is compatible with an edge-on adsorption, while for TDC and TD0, the thickness of the adsorbed layer is twice the thickness expected for flat-on adsorption. The exciton interaction extracted from the steady-state spectroscopy of the adsorbed dyes is much smaller than observed for H- or J-aggregates of the same dyes in solution or adsorbed to other surfaces such as Langmuir films or silver halides. For TDC, TD2 and TD0, the values of the exciton interaction are compatible with a close packed flat-on adsorption. Hence, optimizing the interaction between the adsorbed dye and hBN rather than between the adsorbed dye molecules governs the packing of the adsorbed dye molecules. The observation of the spectral shifts attributed to the exciton interaction at low average coverage of the hBN surface indicates that the exciton interaction already occurs at low coverage of the hBN surface. This observation is in agreement with the AFM micrographs, which show clustering of the the adsorbed dye molecules already at low coverages.

1. INTRODUCTION

Recently, hexagonal boron nitride (hBN) was proposed as a platform to study the light-matter interaction for molecules adsorbed on its surface.[1] hBN is an inorganic material consisting of an equal number of boron and nitrogen sp^2 hybridized atoms placed in an alternating order to form a honeycomb lattice and is characterized by a lattice parameter of 0.25 nm. Besides being iso-structural to graphene, hBN is also iso-electronic to graphene since boron and nitrogen are direct neighbors of carbon in the periodic table. The electrons of the B-N bonds are preferentially confined to the nitrogen atom due to their electronegativity. Hence the σ-

bond is polarized, and the lone pair electrons in the p_z orbital of the nitrogen are partially delocalized to the empty p_z orbital of boron causing an inefficient π-bond between boron and nitrogen.[2,3] Multilayer formation, where a boron atom is located on top of a nitrogen atom and vice versa, is possible thanks to van der Waals forces and is characterized by an interlayer distance of 0.33 nm.[4,5] As an electrically insulating two-dimensional (2D) material with an energy bandgap of 5.5 eV, supported hBN has potential applications in photo- and electro catalysis, but also as a platform to investigate light-matter interactions since it will decouple the adsorbate from the underlying substrate. Besides this, hBN is also an interesting material to study the organization of molecules,[6–12] and has been shown to be stable in various liquids and under electrochemical conditions.[13,14]

This prompted us to study how the adsorption of some thiacarbocyanine dyes given in table 1 on hBN affects their spectroscopic and photophysical properties. More specifically, the adsorption of several thiacarbocyanine dye molecules on hBN was studied by means of steady-state spectroscopy and atomic force microscopy.[1,11,12,15–17]

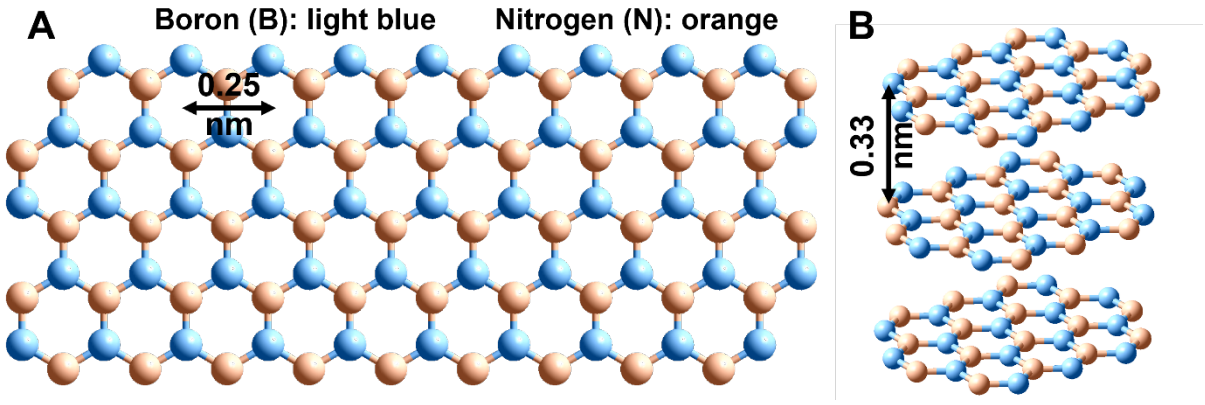

Figure 1 A Monolayer hBN and B multilayer formation.

In solution the presence of two isomers (all-*trans* EEEE and mono-*cis* EEZE) of thiacarbocyanine dyes has already been investigated.[18–20] The equilibrium between both isomers is determined by the presence of substituents on the meso (9), 3-3' and 5-5' positions. In the ground state, the substitution of the meso-position will be the dominant factor determining the position of this equilibrium. While for meso-unsubstituted isomers only around 5% mono-*cis* isomer is present, this isomer prevails for meso-substituted cyanines where

steric hindrance of the (bulky) substituents destabilizes the all-*trans* form. One should note however that for meso-ethyl substituted dyes less mono-*cis* is present than for meso-methyl substituted dyes.[18] In the excited state increasing the bulkiness of the substituents in the 3-3' position has been shown to decrease the rate constant for internal conversion or cis-trans isomerization slowing down torsional movements by viscous friction.[21,22] This will increase the efficiency of radiative decay (fluorescence quantum yield) and the excited state decay time upon increasing the size of the substituents in the 3-3' position for both the all-*trans* and mono-*cis* isomers. The size of the 3-3' substituents does not influence the features and maxima of the stationary spectra. The presence of substituents (Cl or Me) on the 5-5' position leads to a redshift of the stationary spectra because of the result of an increase of the size of the conjugated system. The latter substituents have however no or little effect on the fluorescence decay times of both isomers.[18] The photophysics of aggregates of thiacarbocyanine dye molecules has already extensively been studied by means of experimental and theoretical work.[23–28]

Table 1 Abbreviations, substitution pattern, counterions and full name of the studied thiacarbocyanine dyes (Et: ethyl, SulfoPro: sulfopropyl, H: hydrogen, Cl: chlorine, $EtSO_4^-$: tosylate anion and $NH(Et)_3^+$: triethylammonium ion).

Dye	3-3'-R	5-5'-R	9-R	Counterion	Full name
TDC	Et	Cl	Et	$EtSO_4^-$	5,5-dichloro-3-3'-diethyl-9-ethyl-thiacarbocyanine
TD2	Et	H	Et	Cl^-	3-3'-diethyl-9-ethyl-thiacarbocyanine
TD0	Et	H	H	Cl^-	3-3'-diethyl-thiacarbocyanine
THIATS	SulfoPro	Cl	Et	$NH(Et)_3^+$	5,5-dichloro-3-3'-disulfopropyl-9-ethyl-thiacarbocyanine

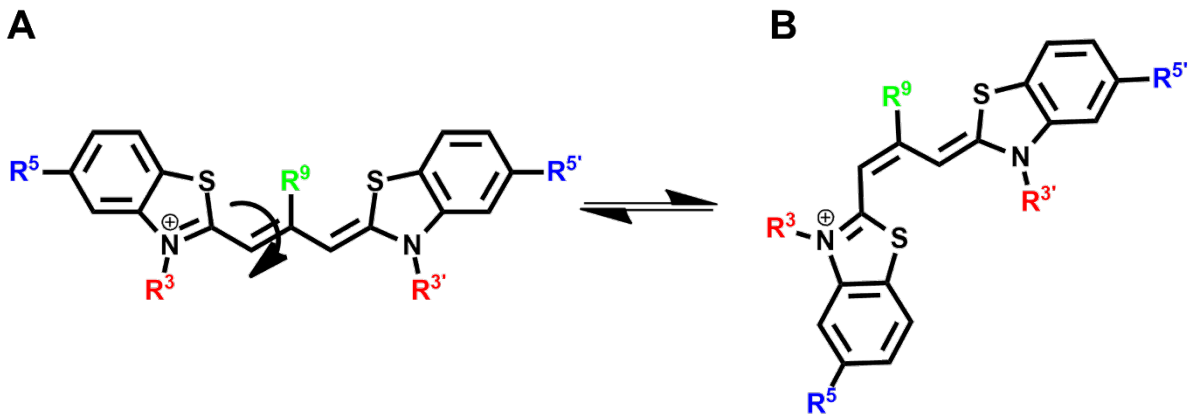

Figure 2 General structure of thiacarbocyanine dyes and its cis-trans isomerization with A the all-*trans* and B the mono-*cis* isomer.

2. MATERIALS AND METHODS

The hBN platelets (multilayers) with lateral size below 5 µm were acquired from Sigma-Aldrich and used without further treatment. The solvents ethanol (Merck, 99.9%), Milli-Q water (Merck, ultrapure) and n-heptane (Sigma-Aldrich, 99%) were used without further purification. The thiacarbocyanine dye TDC was a gift from Agfa, while TD2, TD0 and THIATS were synthesized in the research group.[18]

The specific surface area of non-exfoliated, bulk hBN material was determined through the Brunauer-Emmet-Teller (BET) analysis. The samples (approximately 100 mg) were heated at 150°C for 10 hours under vacuum before recording nitrogen adsorption/desorption isotherms using a Micromeritics 3Flex set-up.

The preparation of the samples of TDC, TD2, TD0 and THIATS in solution and adsorbed on hBN for steady-state spectroscopy measurements and the determination of their molar extinction coefficient and adsorption isotherm are described in the supplementary information (SI).

UV-visible absorption spectra of dilute solutions were recorded using a Perkin Elmer Lambda40 spectrophotometer in quartz cuvettes with path length of 1 mm and 1 cm resp. for the construction of the adsorption isotherms and to study the behavior of dyes in solutions. The absorption spectra were collected with blank corrections. The emission and excitation spectra of the dyes adsorbed on hBN were determined with a Horiba Jobin Yvon Fluorolog 3 spectrofluorometer in front-face configuration, while in solution they were recorded in right-angle configuration. The excitation spectra were corrected for the wavelength dependence of the intensity of the excitation light for temporal fluctuations of this intensity. The emission spectra were corrected for the wavelength dependence of the detection channel throughput and the sensitivity of the detector.

The dye:hBN:silicon samples were studied using atomic force microscopy (AFM) on a Cypher ES (Asylum Research) system at 32°C. The topography images were extracted using the

tapping mode at the air/substrate interface using OMCL-AC240TS-R3 probes (Olympus Corporation, spring constant ~2 N/m, resonance frequency ~70 kHz) for blank measurements in absence of dye molecules and using Arrow-UHFAuD probes (Nanoworld, spring constant ~2 N/m , resonance frequency ~1500 kHz) for dye measurements on hBN covered with the adsorbed dyes. The same tip was used to scratch away the dye layer in the contact mode at a constant force (100 nN) to determine the thickness of the adsorbed dye layer. All SPM images were analyzed and processed using Scanning Probe Imaging Processor (SPIP 6.3.5) software from Image Metrology ApS.[29]

Molecular mechanics simulations were performed using HyperChem 8.0.8 software (Hypercube, Inc.) for both all-*trans* and mono-*cis* isomers of TDC and TD0 molecules adsorbed on hBN. Their molecular mechanics calculations with the MM+ force field used the Polak-Ribière conjugate gradient algorithm, which is implemented in this software to a convergence of gradient of 0.2 kcal $Å^{-1}$ mol^{-1}.[30]

3. RESULTS AND DISCUSSION

3.1. Specific Surface Area of Boron Nitride Platelets

The specific surface area of non-exfoliated hBN platelets can be roughly estimated, starting from the density (2.29 g/cm^3) and assuming that only the sheet-like top and bottom faces of the platelets are available for adsorption and that the hBN surface is not porous. According to the information provided by the supplier, which states that the lateral dimensions of the hBN platelets are below 5 µm, the maximum top face area of one platelet is 25 $µm^2$. Using the experimentally observed thickness, obtained by AFM on non-exfoliated platelets (around 0.15 µm)[31], a specific surface area on the order of 15 m^2/g can be expected. A more accurate experimental determination of the specific surface area can be achieved through a Brunauer-Emmett-Teller (BET) analysis[32,33] on three hBN samples using nitrogen (N_2) gas at 77K. The results of these measurements are summarized in table 2. The nitrogen adsorption/desorption isotherms are provided in the SI (figure S1). The average BET specific surface area s_{BET} of

the hBN platelets was found to be equal to 11±2 m^2/g, which is of the same order of magnitude of the initial estimate of 15 m^2/g. Having established the surface area, it becomes possible to quantitatively evaluate the surface density of the adsorbed dye molecules on the surface of hBN platelets.

Table 2 Specific surface area data of hBN nanoplatelets as determined from BET.

Sample	BET specific surface area (m^2/g)
1	13.0
2	7.9
3	11.3

3.2. Determination of the Maximum Number of Molecules Adsorbed onto the hBN Surface

In order to determine the adsorption isotherms, the molar extinction coefficients (ε) of the dyes used were determined in an ethanol:water (EtOH:H_2O) (1:1) mixture (table 4) using the procedure given in the SI.

The absorption spectra were determined for several concentrations of the dye molecules and the absorbance at the maximum was plotted versus the concentration (figure S2). Fits of the absorbance versus concentration yielded a linear relationship for all dyes with a correlation coefficient (R^2) of 0.997 and allowed to obtain their molar extinction coefficient. This adherence to the law of Lambert-Beer suggests that in the concentration range (from 10^{-6} M to $3x10^{-4}$ M) used no major aggregation of the dyes occurs in EtOH:H_2O (1:1). Compared to the molar extinction coefficients reported in methanol (MeOH)[18], the results obtained in EtOH:H_2O (1:1) differ to a small extent for TDC, TD2 and TD0. This could possibly be due to a shift of the equilibrium between the all-*trans* and mono-*cis* isomer. The molar extinction coefficient of TDC (1.20±0.02 L mol^{-1} cm^{-1}) is 25% larger than the molar extinction coefficient of TD2 (0.92±0.02 L mol^{-1} cm^{-1}) indicating that the chlorine atoms only induce a minor increase of the transition dipole.

By measuring the absorbance of a known volume (≈ 3mL) of the dye solutions before the addition of hBN powder and of the supernatant after addition of hBN and centrifugation (see

experimental procedure in SI), and using the molar extinction coefficient of TDC, TD2, TD0 and THIATS the change in concentration of the dye solution by adsorption of the dyes to hBN could be determined. This allowed us to calculate the number of dye molecules that are immobilized on the hBN surface after the addition of hBN to the initial dye solution (details see SI). Combining these data with the specific surface area of 11±2 m^2/g of the hBN platelets (*cfr. supra*) allows us to plot the surface density of the adsorbed dye molecules versus the initial dye concentration rendering the adsorption isotherm of TDC, TD2, TD0 and THIATS on hBN (figure 3). The adsorption isotherms are then fitted to the Langmuir-Freundlich-Sips (LFS) (equation 1 (eq. 1)), which is used to describe the adsorption from dilute adsorbate solutions on a surface. Contrary to the simple Langmuir isotherms, the LFS model takes into account that the adsorption sites are not necessarily equivalent and that interactions between adsorbates at the surface occur.[32–34]

$$Q_e = Q_{Sat}\frac{(K_{LFS}c)^n}{1+(K_{LFS}c)^n} \qquad \text{Eq. 1}$$

In equation 1, Q_e is the number of molecules adsorbed on the surface per unit area at equilibrium (surface density), Q_{Sat} is the maximum possible number of adsorbed molecules per unit area, c is the initial adsorbate concentration in solution, n is a measure for heterogeneity and cooperativity (n = 1 for a homogeneous material in the absence of cooperativity) and K_{LFS} is the LFS constant (an affinity constant for adsorption).

Table 3 Data obtained via fitting the adsorption isotherms of the studied thiacarbocyanine dyes with the LFS method. ID is the intermolecular distance (length of one molecule of TDC and THIATS is 2.1 nm and of TD2 and TD0 1.9 nm) recovered from Q_{Sat}.

Dye	Q_{Sat} (m^{-2})	K_{LFS}	n	R^2	ID (nm)
TDC	$5.24\pm0.24\times10^{17}$	$1.05\pm0.28\times10^{5}$	1	0.888	0.91
TD2	$4.77\pm0.16\times10^{17}$	$3.76\pm0.44\times10^{4}$	1	0.961	1.10
TD0	$8.67\pm0.27\times10^{17}$	$6.15\pm0.90\times10^{4}$	1	0.985	0.61
THIATS	$1.02\pm0.03\times10^{18}$	$3.13\pm0.31\times10^{4}$	1	0.981	0.45

The adsorption isotherms of the studied thiacarbocyanine dyes all show similar features (figure 3). A steep increase of the surface density of the adsorbed dye molecules with increasing concentration of the dye solutions is followed by leveling off to saturation. The values of the

correlation coefficient (R^2), which is always close to 1, suggest that the experimental results fit the LFS adsorption isotherms. The maximum number of molecules that adsorb on the surface of hBN per unit area (Q_{Sat}) is for TDC, TD2, TD0 and THIATS in the same order of magnitude ($5x10^{17}$ to 10^{18} m^{-2}). While for TDC and TD2 the values for Q_{Sat} that are obtained are similar within experimental error, the values obtained for TD0 and especially THIATS are significantly larger. Due to the absence of chlorine atoms and a meso-ethyl group, TD0 is expected to have a smaller size allowing a larger value of Q_{Sat}. Unexpectedly, the values of Q_{Sat} obtained for THIATS, the molecule with the largest size, are larger than those found for the other molecules. These results were confirmed when repeating the determination of the adsorption isotherms. These data suggest that for THIATS at least a partial edge-on adsorption must be considered in contrary to the other cationic molecules. THIATS is a zwitterion with a negative charge, which could influence the interaction between the dye and the surface (van der Waals interactions, ion-dipole interactions and dipole-dipole interactions). While it is evident that changing the net charge of the dye will affect K_{LFS}, the observed increase of Q_{Sat} indicates that changing the net charge of the dye and the presence of negative end groups on the 3-3' substituents also leads to the formation of multilayers or a different orientation (*cfr. infra*) of the adsorbed THIATS molecules.

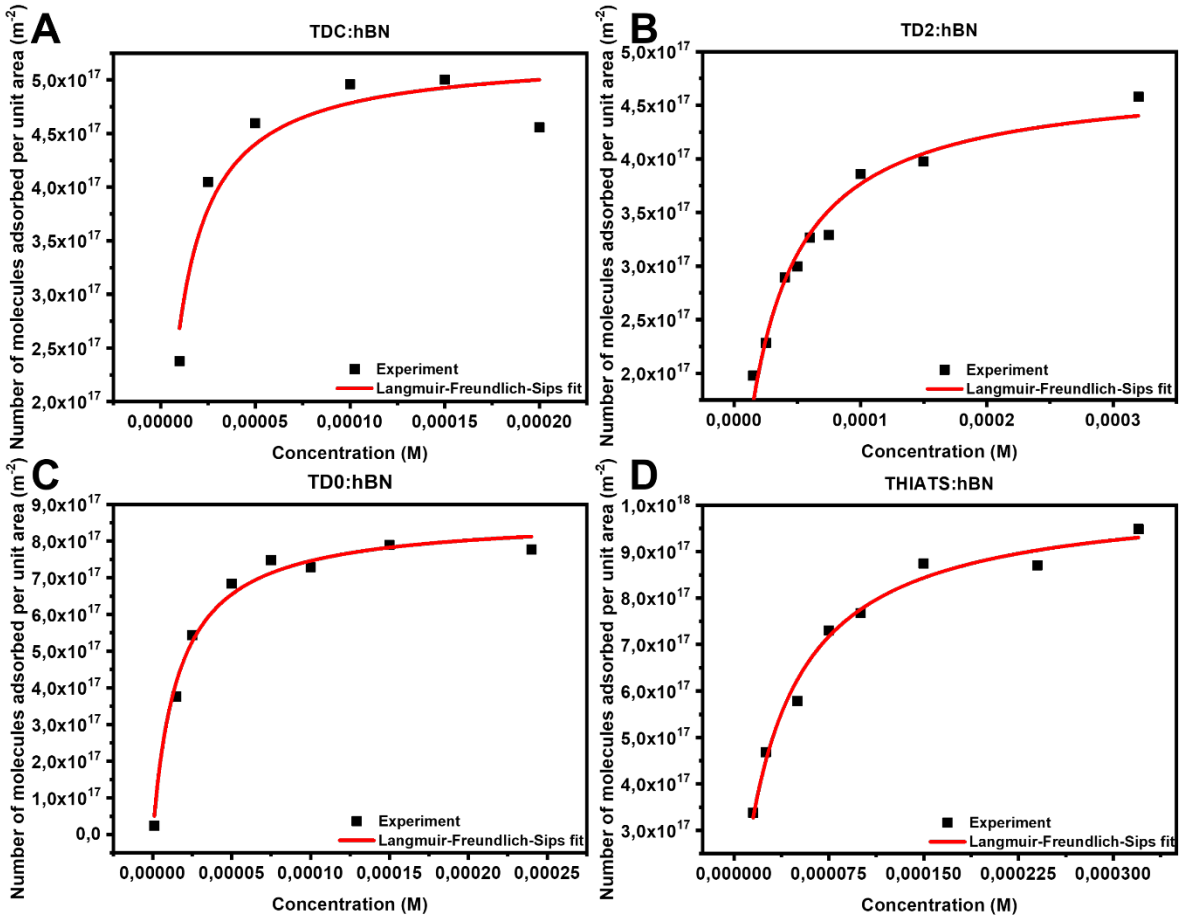

Figure 3 Adsorption isotherms of A TDC, B TD2, C TD0 and D THIATS adsorbed on the surface of hBN and fitted to the LFS isotherm.

From the values of Q_{Sat} and taking into account that the length of one molecule of TDC, TD2, TD0 and THIATS amounts to respectively 2.1, 1.9, 1.9 and 2.1 nm,[35] it is possible to calculate the intermolecular distance of the adsorbed molecules at maximum coverage. This distance amounts to 0.91, 1.10, 0.61, 0.45 nm for respectively TDC, TD2, TD0 and THIATS. This suggests that TDC and TD2 adsorb flat-on with their molecular plane parallel to the boron nitride surface rather than edge-on. Here one should note that molecular mechanics calculations (see SI) also suggest flat-on adsorption with similar intermolecular distances for TDC and TD0. On the other hand, for THIATS, where a value of 0.45 nm is obtained, at least partial edge-on adsorption is more likely. In the case of a completely edge-on adsorption, one would expect an intermolecular distance of 0.36 nm taking into the account the molecular dimensions for a close packing of the adsorbed molecules.[35–37] This would also imply that TDC and TD2 adsorb on the hBN surface with their molecular plane parallel to the boron nitride

surface while THIATS adsorbs rather edge-on. Previous literature reports suggest edge-on adsorption of cyanine dyes on Langmuir films and silver halides,[25,38,39] while for other cyanine dyes an edge-on adsorption on mica was observed.[40,41] When comparing the values of K_{LFS}, the larger value of K_{LFS} observed for TDC versus TD2 can be attributed to the presence of the polarizable Cl-atoms and the polar C-Cl bond leading to stronger van der Waals and dipole-dipole interactions with the hBN substratum.[42,43]

In order to gain further insight into the aggregation of TDC, TD2, TD0 and THIATS on hBN, AFM and steady-state spectroscopy experiments of the adsorbed dyes were performed.

3.3. Visualization of the Behavior of the Thiacarbocyanine Dyes on hBN using AFM

In order to get more information on the possible self-assembly of the adsorbed dye molecules AFM micrographs were obtained for hBN flakes to which dye molecules were adsorbed. Samples with different concentrations of the initial dye solutions were prepared via the sample preparation method discussed in the SI. These experiments require large flakes with a size of about 20-50 µm. Furthermore, these flakes should have a flat surface in order to visualize height differences caused by the deposition of the adsorbed molecules. The micrographs displayed in figure 4 show that the flake size is around 20 µm and that between two consecutive step edges there is a flat area of 1 to 2 µm. Hence, the experimental procedure discussed in the SI allows obtaining flakes suitable to study the adsorption of the cyanine dyes by AFM. According to the cross section shown in figure S3, the “flat” areas show fluctuations of less than 0.2 nm while the step edge amounts to 0.4 to 0.6 nm. This is slightly larger than the thickness of the hBN layer which equals 0.33 nm.[4,5]

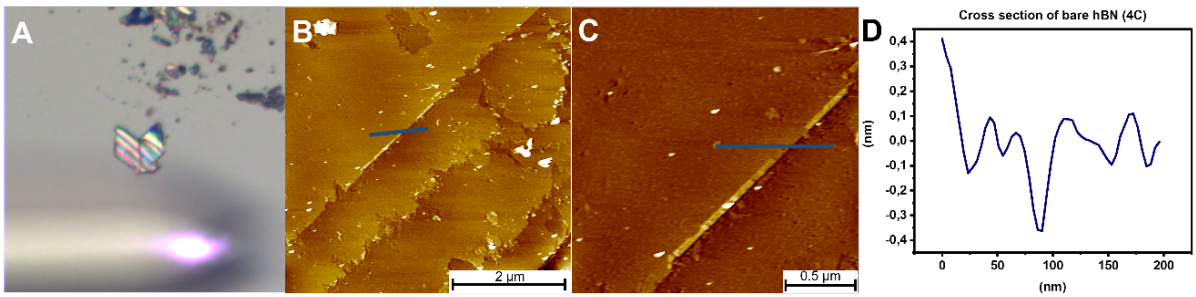

Figure 4 Bare hBN flakes on a Si/SiO_2 wafer. A transmission microscopy image of an hBN flake, B topographic AFM images of hBN flakes showing the step edges, C zoomed image of a step edge and D cross section of 4C along the blue line are given in figure S3. It is possible that the white dots in figure 4B and 4C are contaminants.

The adsorption isotherm of TDC (figure 3A) indicates that saturation starts for adsorption from a dye solution with an initial concentration around $25x10^{-6}$ M. Under these conditions according to figure 3A and table 3 about 72% of the hBN surface is covered by adsorbed dye molecules. Therefore, this concentration was chosen to study the morphology of the adsorbed dye layer with AFM. Comparing figures 5A and 5B to figures 4B and 4C, figures 5A and 5B clearly shows that most of the hBN surface is covered by clusters of grainy structures with a size less than 10 nm, which are formed by the dye adsorption. There is however no indication of further long range ordering. These clusters are separated by small irregularly shaped lower domains, probably corresponding to uncovered hBN. These micrographs also show that for adsorption from a $25x10^{-6}$ M solution the experimental procedure followed does not lead to the formation of large microcrystals by evaporating dye droplets. According to figure 5E, 5F, and figure S4, the height of the grainy structures is about 0.4 to 0.5 nm, which is slightly more than what is expected for a monolayer (0.36 nm). In order to get more information on the height of the adsorbed layer a square area of 0.2 x 0.2 nm was scratched in contact mode with a force of 100 nN (figure 5C). When the adsorbed dye is removed by scratching, a uniform flat area becomes visible. The “vertical” cross section (figure S4) shows that the scratched area is about 0.5 to 0.6 nm below the unscratched one. In the “horizontal” cross section the rims caused by the removed material becomes visible. A height histogram of the scratched area and its surroundings (figure 5D) shows a bimodal distribution with the green and orange maxima corresponding to respectively the scratched area and its surroundings. The distance between

the maxima amounts to 0.8±0.1 nm, which is at least twice the thickness of a flat-on adsorbed TDC molecule. It is however smaller than the height of an edge-on adsorbed molecule, which is about 1 nm.[35–37] Lowering the concentration to $1x10^{-6}$ M of the initial TDC solution where according to its adsorption isotherm the hBN surface coverage should be around 9%, we observe similar clusters of grainy structures (figure S5), which now however only occupy a small fraction of the hBN surface. According to the corresponding cross-section (figure S5), the height of the adsorbed layer amounts to 0.7 nm. Besides these agglomerated grainy structures, one can also see a sparse distribution of isolated grains with a size of 20 nm or less and a similar height as the clusters. These grains are much larger than a single dye molecule for which a size of 1x2 nm would be expected. The distance between those grains or between the grains and the larger cluster is at least several tens of nm. Figure S5 gives no indication for a homogeneous distribution of isolated dye molecules. Even at low overall coverage, the adsorbed dye molecules already assemble to form grains and clusters of grains. Although AFM cannot exclude that there are isolated adsorbed dye molecules as the latter would possible not be observable by AFM, the shift of the excitation and emission spectra (*cfr.* infra) indicates that even at low coverage most adsorbed molecules are aggregated. One should note that this clustering occurs only for adsorbed dyes on the surface and that there is no indication that aggregates preformed in solution are adsorbed. The linear plots of absorbance versus concentration (figure S2) indicate that for the solvent system used no dye aggregation occurs in solution up to a concentration of $250x10^{-6}$ M.

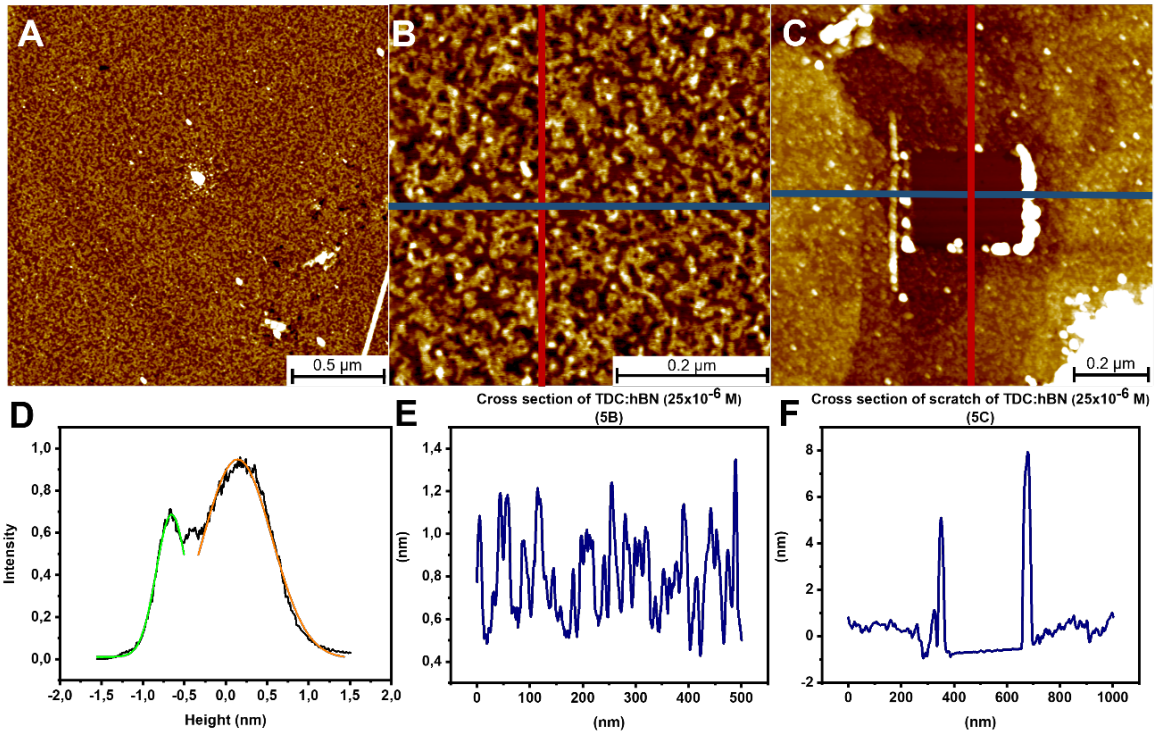

Figure 5 Topographic AFM images of TDC adsorbed on the surface of hBN from a solution with an initial dye concentration of $25x10^{-6}$ M for an image area of 2 µm (A) and 500 nm (B). C Topographic AFM image of the scratch area and its surroundings. D height histogram of the scratched area and its surroundings. Cross sections along the blue line in 5B and C are given in 5E and 5F. Cross sections along the red line in figure 5B and 5C are given in the SI.

The AFM micrographs of TD0 molecules (figure 6A and 6B) adsorbed from solution with an initial concentration of $1x10^{-6}$ M on the surface of hBN consists of small granular structures of at least 10 nm diameter, which sometimes assemble to oligomers. The fraction of the surface covered by the structures is much smaller than 50%. These grainy structures are much larger than individual molecules, with a size of 1x2 nm, indicating that even at $1x10^{-6}$ M, where only a small fraction of the surface is covered by adsorbed TD0 molecules, aggregation and self-assembly occur in analogy to the observations made for TDC. In contrast to TDC, no large clusters of the grainy structures separated by nearly uncovered hBN are observed. Upon adsorption from a $25x10^{-6}$ M solution, a more uniform coverage with randomly distributed "holes" is observed (figure 6D and 6E). While the height of the grainy structures is about 1.0 to 1.2 nm, a similar depth of the holes is seen in figure 6C and 6F and in figure S6. This is

about three times the thickness of a monolayer of flat-on adsorbed molecules and more than the height of edge-on adsorbed molecules.

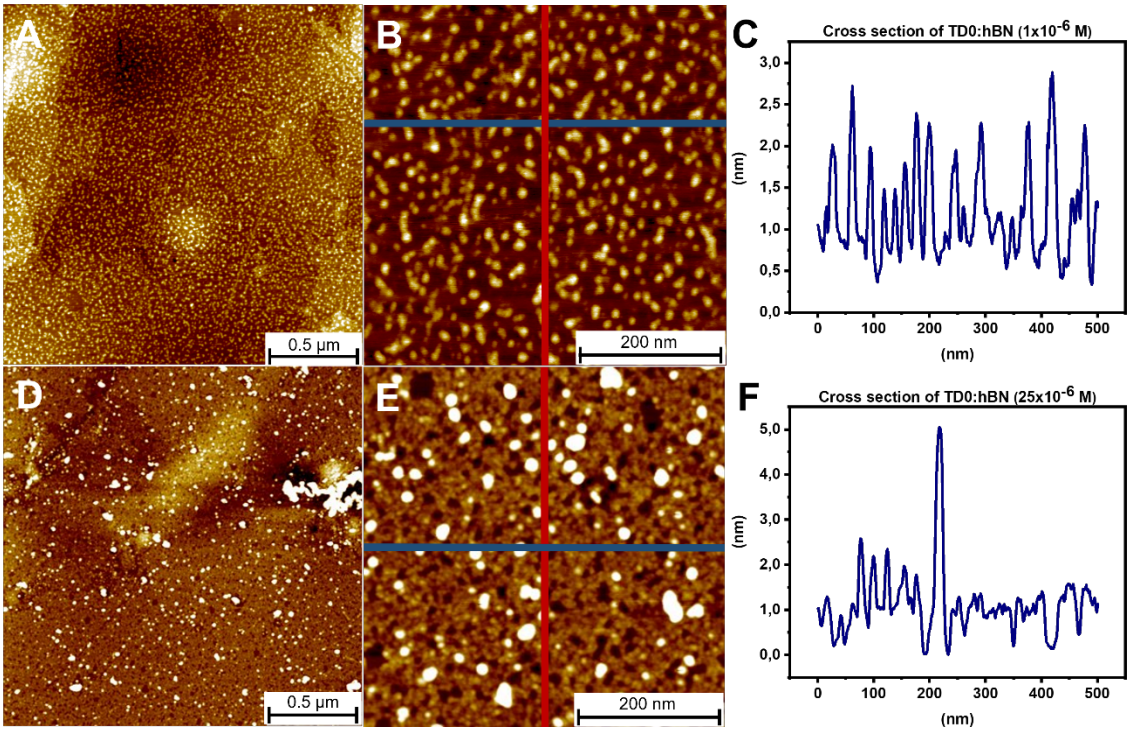

Figure 6 Topographic AFM image of TD0:hBN adsorbed from a $1x10^{-6}$ M TD0 solution (A and B) with the corresponding cross section along the blue line in 6B (C) and from a $25x10^{-6}$ M TD0 solution (D and E) with the corresponding cross section along the blue line in 6E (F). Cross sections along the red line in 6B and 6E are given in the SI.

Contrary to TDC and TD0 no grainy nm size structures are observed for THIATS adsorbed on hBN from a $1x10^{-6}$ M (figure 7A) or $10x10^{-6}$ M (figure 7B) solution. We rather observe continuous patches with a large number of nm size pinholes. Upon increasing the dye concentration in the solution, the fraction of the surface covered by these patches becomes larger. Some of the larger particles visible in the topography image (figure 7B) can be identified as hBN flakes from the phase image (figure S8B), which indicates differences in interaction with the AFM tip. The height of the adsorbed layer (figure 7C) or the depth of the “holes” is about 1 nm, which corresponds to the height of edge-on adsorbed molecules. As observed for TDC and TD0 the resolution of the micrographs gives no indication about the packing on molecular level or on long-range order of the adsorbed dye molecules.

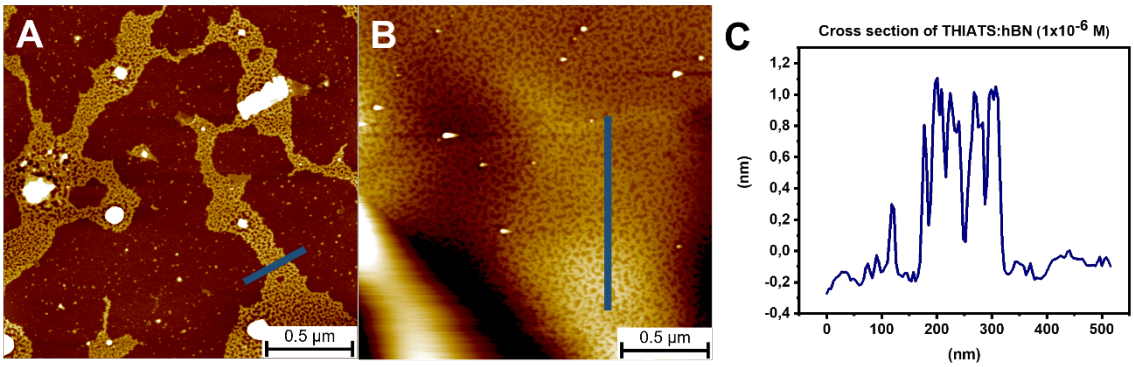

Figure 7 Topographic AFM image of THIATS:hBN composites with resolution of 2 µm with adsorption from a A $1x10^{-6}$ M and B $10x10^{-6}$ M solution. Cross section along the blue line in 7A is given in 7C, while the cross section along the blue line in 7B is given in the SI.

For all dyes used the AFM experiments indicate that while at sufficiently high concentration (≥ $10x10^{-6}$ M) a more or less uniform dye layer (with some holes) is adsorbed, this layer only covers part of the hBN surface at low dye concentrations ($1x10^{-6}$ M). None of the AFM experiments suggests the formation of larger microcrystals related to evaporation of remaining droplets of the dye solution. The AFM experiments also indicate that for all dyes clustering rather than a random distribution of individual molecules occurs already at low dye concentration where only a small fraction of the hBN surface is covered by the dye. Already at a low coverage patches of clustered dye molecules are formed, which are separated by uncovered hBN. For THIATS, the thickness of the adsorbed layer agrees with the density of a layer of edge-on adsorbed molecules suggested by the adsorption isotherm. For TDC and TD0, the thickness of the adsorbed layer is twice as large as what would be expected for flat-on adsorbed molecules as suggested by the density at saturation of the adsorption isotherm or the molecular mechanics simulations (*cfr. infra*). While this could suggest that for TDC and TD0 at least part of the adsorbed dye layer is a multilayer, this hypothesis is not compatible with the values of Q_{Sat} obtained from the adsorption isotherms.

3.4. Steady-State Spectroscopy in Solution

The spectroscopy of the thiacarbocyanine dyes, which are prone to aggregation, was already extensively investigated in solution[18] (MeOH) as well as adsorbed on self-assembled[16] or Langmuir films[17,25]. Due to the similarity between the earlier investigated steady state,

spectroscopy of the dyes dissolved in MeOH and the spectra obtained in an EtOH:H_2O (1:1) mixture, the spectra in EtOH:H_2O (1:1) will only be discussed summarily.

The absorption, excitation and emission spectra of the investigated dyes in EtOH:H_2O (1:1) show a vibrational structure with a maximum and a respectively blue- or redshifted shoulder corresponding to resp. 0-0 transition and 0-1 vibronic transition (figure S10 and S11). The maxima and width of absorption, excitation and emission spectra and the Stokes shift between the excitation and emission spectra are given in table 4. To ensure that the values given for the width of the excitation and emission bands only reflect the width of the 0-0 transition (determined by low frequency vibrations), the values $FW_{2/3}$ rather than FWMH are given. TDC and THIATS show a redshift of the absorption, excitation and emission spectra with respect to those of TD2 due to the presence of the chlorine atoms, which extend the conjugated system. The substituents on the 3-3' positions do not exert an influence on the conjugated part of the molecules and hence on the stationary spectra. Therefore, the absorption, excitation and emission maximum of TDC are similar to those of THIATS.[18,19] This was expected as the substituents on the 3-3' positions do not exert an influence on the conjugated part of the molecules and hence on the stationary spectra. The absorption spectrum of TD0 is even further redshifted and narrower, which at first glance could be attributed to the absence of the steric hindrance of the meso-alkyl group resulting in an increased planarity.[36,44] However one should note that while for TD0 the maxima of absorption and excitation spectra are within experimental error identical, the latter are shifted 10 to 12 nm to longer wavelengths for the other dyes. In analogy to what was concluded by Vranken *et al.*[18] for the same dyes dissolved in MeOH, this could be related to the presence of the all-*trans* and mono-*cis* isomers. While for TD0 the absorption, excitation and emission spectra can be attributed to the all-*trans* isomer, the absorption spectrum of the other dyes is a combination of that of the all-*trans* and mono-*cis* isomers, while the excitation and emission spectra are mainly those of the all-*trans* isomers. This discrepancy is due to the significantly larger fluorescence quantum yield of the all-*trans* isomer versus that of the mono-*cis*. This also explains why $FW_{2/3,Abs}$ of TDC, TD2 and

THIATS is significantly larger than $FW_{2/3,Abs}$ of TD0 and why $FW_{2/3,Abs}$ of these dyes are significantly larger than their $FW_{2/3,Em}$. This means that the Stokes shift of TDC, TD2 and THIATS should be calculated from the shift between the maxima of the excitation and emission spectra. When the Stokes shift is obtained in this way one observes that similar values are found for the four dyes suggesting that the four all-*trans* isomers are planar and sterically unhindered. The latter is also reflected in the similar values of $FW_{2/3,Exc}$ obtained for the four dyes.

Table 4 Spectral data of TDC ($10x10^{-6}$M), TD2 ($1x10^{-6}$ M), TD0 ($15x10^{-6}$M) and THIATS ($1x10^{-6}$ M) in EtOH:H_2O (1:1) with S the Stokes shift and $FW_{2/3}$ the band width at 2/3 of the maximum. $FW_{2/3}$ rather than FWMH is used to reduce the contribution of the 0-1 transition. a emission from 570 to 600 nm, b emission form 560 to 590 nm, c emission from 565 to 595 nm, d emission from 570 to 600 nm.

Dye	λ_{Abs} (nm)	ε ($Lmol^{-1}cm^{-1}$) EtOH:H_2O (1:1)	λ_{Em} (nm)	λ_{Exc} (nm)	S (cm^{-1})*	$FW_{2/3, Abs}$ (cm^{-1})	$FW_{2/3, Em}$ (cm^{-1})	$FW_{2/3, Exc}$ (cm^{-1})
TDC	552	$1.20\pm0.02x10^5$	580	562[a]	550±50	920±50	600±50	670±50
TD2	547	$0.92\pm0.02x10^5$	571	557[b]	440±50	1000±50	730±50	650±50
TD0	559	$1.05\pm0.02x10^5$	574	558[c]	500±50	620±50	720±50	880±50
THIATS	554	$0.86\pm0.02x10^5$	579	566[d]	400±50	980±50	650±50	600±50

*The Stokes shift was calculated between the maxima of the excitation and emission spectra.

3.5. Steady-State Spectroscopy Adsorbed on the Surface of hBN

While it was possible to obtain reliable fluorescence and excitation spectra for the adsorbed dyes, no reliable absorption spectra could be obtained. The steady-state fluorescence spectra obtained upon excitation at 525 nm of TDC, TD2, TD0 and THIATS adsorbed on hBN are shown in figure 8 for different initial concentrations of the dye in the solution from which the adsorption occurred. As observed in solution, the emission spectra of the thiacarbocyanine dyes adsorbed on the surface of hBN show a vibrational structure with a peak and a redshifted shoulder corresponding to resp. the 0-0 and 0-1 transition. The emission maxima and the $FW_{2/3}$ are given in the SI (table S6). The excitation spectra of the thiacarbocyanine molecules adsorbed on hBN were recorded for an initial dye concentration ranging from 10^{-7} M to 10^{-3} M at detection wavelengths (λ_{Det}) 603 nm and 630 nm for TDC, TD2 and TD0 and at 610 nm, 615 nm and 630 nm for THIATS (spectra are provided in SI). These detection wavelengths

were used instead of the emission maxima to decrease the effect of stray light on the spectra. Emission and excitation spectra obtained for concentrations of the initial dye solution exceeding $240x10^{-6}$ M should be considered with caution as they can be disturbed by crystals forming upon drying of the remaining dye solution. The excitation spectra for the different dyes, different coverages and emission wavelengths are given in the SI (figure S12 to S15) while their maxima are shown in table 5. One should note that the excitation spectra are within experimental error independent of the emission wavelengths used.

Already at the lowest two dye concentrations, where the coverage is only 2%, a redshift of the emission spectra of the adsorbed dyes (versus solution) is observed, which amounts to 10 nm (300 cm^{-1}) for TDC and TD2, while for TD0 and THIATS this redshift is resp. 20 nm (600 cm^{-1}) and 19 nm (550 cm^{-1}). While for TDC, TD2 and THIATS the values of $FW_{2/3,Em}$ are within experimental error equal to those obtained in solution, $FW_{2/3,Em}$ increases for TD0 from 720±50 cm^{-1} in solution to 900±50 cm^{-1} adsorbed on hBN. Under the same conditions the maxima of the excitation spectra of TDC and TD2 show no shift compared to those obtained in solution, while those of TD0 and THIATS show a redshift of 15 nm (470 cm^{-1}) and 14 nm (430 cm^{-1}). Hence, while for TDC and TD2 the Stokes shift (between excitation and emission spectra) increased by about 300 cm^{-1} to 800 cm^{-1}, it increased by about 100 cm^{-1} for TD0 and THIATS, which is at the limit of our experimental precision. The different adsorption behavior of TD0 and THIATS compared to TDC and TD2 suggested by the values of Q_{Sat} obtained from the adsorption isotherms and the AFM micrographs is retrieved in the excitation and emission spectra of the adsorbed dyes.

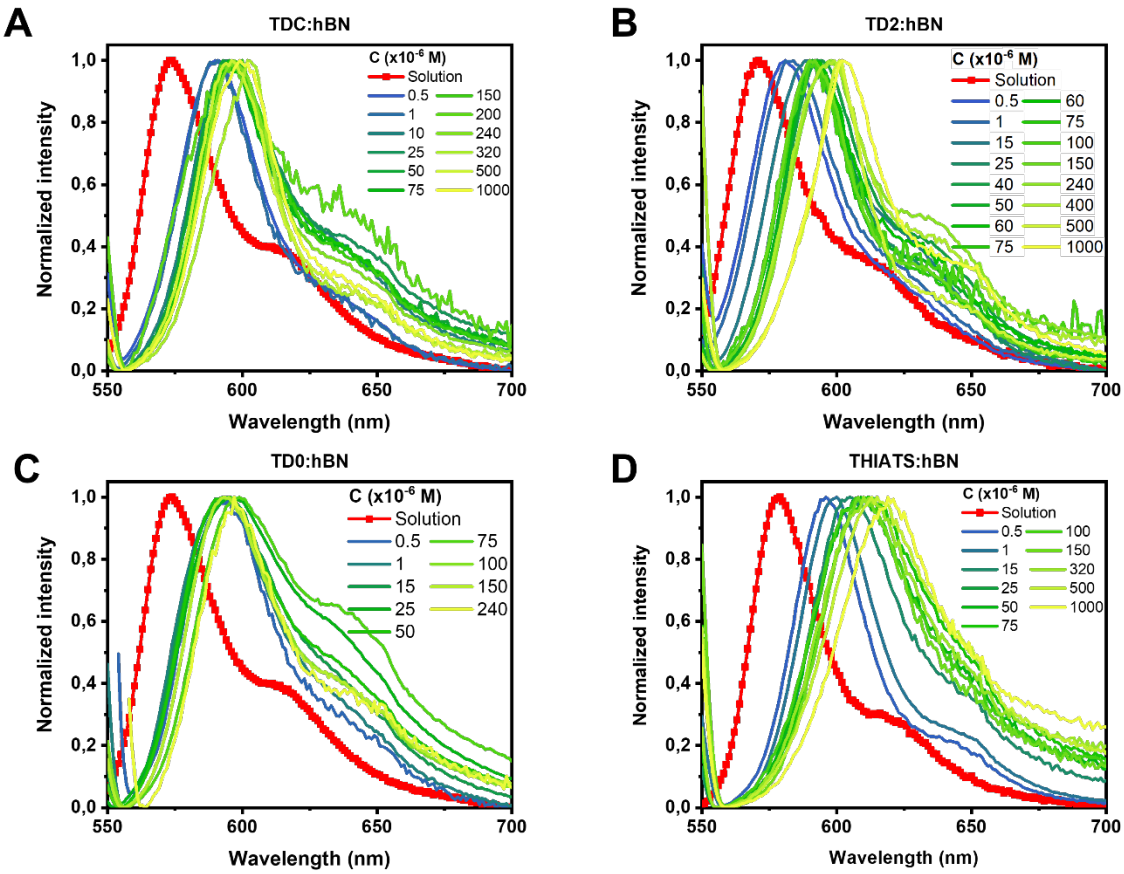

Figure 8 Emission spectra of A TDC B TD2 C TD0 and D THIATS adsorbed on the surface of hBN with increasing initial dye solution concentration. Red squares give the emission spectra of the corresponding thiacarbocyanine dyes in solution. Excitation wavelength was 525 nm.

For TDC, TD2 and to a smaller extent for THIATS the excitation maximum undergoes a further redshift upon increasing the dye concentration in solution and hence the coverage as noted in table 5. This increase of the redshift amounts about 6 to 11 nm (150 to 350 cm^{-1}) at a dye concentration in solution of $200x10^{-6}$ M where the adsorption approaches saturation. For these dyes, the emission maximum undergoes an analogous redshift upon increasing the dye concentration in solution and hence the coverage as noted in figure 8 and table S6, which eventually amounts about 10 nm (300 cm^{-1}) at a dye concentration in solution of $200x10^{-6}$ M where the adsorption approaches saturation. Considering the worse quality (due to scattered light) of the excitation spectra versus the emission spectra the further redshifts of the maxima of the excitation spectra do not differ significantly for these three dyes and match those of the emission spectra. On the other hand, for TD0, no outspoken increase of the redshift of the

excitation or emission spectra is observed upon increasing the dye concentration in solution and hence the coverage of the hBN flakes. For TDC and TD2, the $FW_{2/3,Em}$ does not change upon increasing the loading, while for TD0 and THIATS an initial increase is followed by a rather erratic behavior. One should note that upon increasing the dye concentration of the initial dye solution, the red tail of the emission spectra as well as the shoulder around 650 nm are enhanced for THIATS. This process, which already starts at a $15x10^{-6}$ M dye solution, suggests that at high dye concentrations, besides the 583 nm emission, also emission of strongly interacting sandwich type dye aggregates or excimers is observed.

Table 5 Excitation maxima observed for TDC, TD2, TD0 and THIATS adsorbed onto the surface of hBN with detection wavelengths a, b, c and d resp. 603 nm, 630 nm, 610 nm and 615 nm.

Concentration $x10^{-6}$ M	TDC		TD2		TD0		THIATS		
	$\lambda_{Exc,max}$[a]	$\lambda_{Exc,max}$[b]	$\lambda_{Exc,max}$[a]	$\lambda_{Exc,max}$[b]	$\lambda_{Exc,max}$[a]	$\lambda_{Exc,max}$[b]	$\lambda_{Exc,max}$[c]	$\lambda_{Exc,max}$[d]	$\lambda_{Exc,max}$[b]
	(nm)	(nm)	(nm)	(nm)	(nm)	(nm)	(nm)	(nm)	(nm)
0.5	566	561	555	555	/	573	/	580	579
1	565	564	556	559	/	572	585	584	585
10	567	565	/	/	/	/	/	/	/
15	/	/	561	560	573	572	586	586	580
25	579	574	568	566	579	572	/	582	582
40	/	/	568	565	/	/	/	/	/
50	578	572	569	569	574	572	/	582	582
60	/	/	564	564	/	/	/	/	/
75	574	573	564	564	577	576	587	585	581
100	575	568	564	565	/	574	583	585	581
150	572	567	568	565	/	574	/	588	582
240	559	567	569	565	/	575	/	/	/
320	556	570	/	/	/	/	/	590	580
500	573	570	/	591	/	594	584	582	583
1000	559	567	/	592	/	576	584	/	/

3.6. Rationalization of the Spectral Shifts

For the shifts of the excitation and emission spectra observed upon adsorption essentially, three phenomena can be responsible

1. A shift of the *cis-trans* equilibrium;
2. Interactions between the adsorbed dye and the hBN surface;
3. Interactions between neighboring adsorbed molecules.

At low coverage, the excitation spectra obtained for TDC and TD2 coincide with those in solution, where the emission is attributed mainly to all-*trans* isomers, while the emission is

shifted 10 nm to longer wavelengths. This makes it unlikely that upon adsorption the equilibrium shifts to the mono-*cis* isomers absorbing and possibly also emitting at shorter wavelengths. Furthermore, in contrast to the experimental results (table S6) one would also expect a large $FW_{2/3}$ for the mono-*cis* versus the all-*trans* isomer. Also for TD0, where already in solution no presence of the mono-*cis* isomer is observed[18], and THIATS shifting the equilibrium to the mono-*cis* isomer is even less likely as for those dyes the redshift is even larger than observed for TDC and TD2.

Taking into account that the refractive index of hBN is 1.85, it will be characterized by a larger polarizability than the EtOH:H_2O (1:1) mixture.[45] Hence, the interaction of the dye with the highly polarizable hBN could possibly explain the redshift of the excitation and the emission spectra.[1,22,46,47] One would however expect that this effect, $\Delta\bar{\nu}_S$ (*cfr. infra*), is similar for the absorption and emission spectra and that it is more outspoken for TDC, TD2 and TD0 that are suggested to have a flat-on adsorption by the value of Q_{sat} and/or the molecular mechanics simulations (*cfr. infra* and see SI) than for THIATS that has possibly an edge-on adsorption. In the latter case, the conjugated system of the dye is farther away from the hBN surface. Hence, although a contribution of $\Delta\bar{\nu}_S$ to the observed spectral shifts cannot be excluded, it cannot be the only relevant factor.

Interactions between neighboring adsorbed molecules can lead to delocalization of the excitation over neighboring molecules and spectral shifts as depicted in scheme 1. Upon decreasing the distance between two molecules, exciton interaction, $\Delta\bar{\nu}_{EC}$, splits the excited state into two states $|+\rangle$ and $|-\rangle$ corresponding to the in-phase and out-of-phase interaction of the transition dipoles.[48–52] The exact geometry determines the size and sign of the exciton interaction ($\Delta\bar{\nu}_{EC}$) (scheme 1). When $\Delta\bar{\nu}_{EC} > 0$, the $|+\rangle$ state is shifted to higher energy and the $|-\rangle$ state is shifted to lower energy, while for a negative $\Delta\bar{\nu}_{EC}$ the opposite happens. Interaction between the electrons of one molecule and the nuclei of the other one and van der Waals type interactions between neighboring dye molecules lead to a further stabilization ($\Delta_1 < 0$ and $\Delta_2 < 0$) of the ground and excited state, which is the same for $|+\rangle$ and $|-\rangle$. As

generally $|\Delta_2| > |\Delta_1|$, Δ_2 - Δ_1 will be negative, which means that the latter type of interactions lead to a similar redshift of the absorption and emission spectrum of both, the |+> and |-> states. When the adsorbed dye molecules have a parallel orientation, which is, considering the molecular mechanics simulations (see SI) a reasonable assumption, the transition dipoles of the aggregating molecules are also parallel, hence the transition dipole to the |+> state, $\vec{\mu}_+^*$, equals $\sqrt{2}\vec{\mu}_M^*$ with $\vec{\mu}_M^*$ the transition dipole of an individual molecule, while for the transition to the |-> state $\vec{\mu}_-^* = 0$. This means that absorption will exclusively occur to the |+> state. The shift of the absorption of the dimer compared to a monomer ($\Delta\bar{\nu}_{ABS,D}$) corresponds to $\Delta\bar{\nu}_{ABS,D} = \Delta_2 - \Delta_1 + \Delta\bar{\nu}_{EC}$, while it becomes $\Delta\bar{\nu}_{ABS,AGG} = \Delta_2 - \Delta_1 + 2\Delta\bar{\nu}_{EC}$ for a very large aggregate where each dye molecule can interact on both sides with its neighbors. Besides these interchromophore interactions, also interactions between the adsorbed dye molecules and hBN can lead to a shift of the absorption and emission spectra ($\Delta\bar{\nu}_s$), which (if any) is probably a redshift considering the large refractive index and hence polarizability of hBN. The latter contribution to the spectral shift can be expected to be the same for absorption, excitation and emission spectra. Hence, the shifts of the absorption of an adsorbed dimer amounts to $\Delta\bar{\nu}_{ABS,DADS} = \Delta\bar{\nu}_s + \Delta_2 - \Delta_1 + \Delta\bar{\nu}_{EC}$ while it amounts to $\Delta\bar{\nu}_{ABS,AGGADS} = \Delta\bar{\nu}_s + \Delta_2 - \Delta_1 + 2\Delta\bar{\nu}_{EC}$ for adsorbed larger aggregates.

As $\Delta\bar{\nu}_s + \Delta_2 - \Delta_1$ is negative, a negative value of $\Delta\bar{\nu}_{EC}$ will always lead to a redshift of the absorption spectrum. As in this case |+> is the lowest excited state, emission will occur from this state and will be shifted to the red compared to a monomer in solution by an energy corresponding to $\Delta\bar{\nu}_{EM,DADS} = \Delta\bar{\nu}_s + \Delta_2 - \Delta_1 + \Delta\bar{\nu}_{EC}$ and to $\Delta\bar{\nu}_{EM,AGGADS} = \Delta\bar{\nu}_s + \Delta_2 - \Delta_1 + 2\Delta\bar{\nu}_{EC}$ for respectively dimers and large aggregates. Hence, the absorption (and also excitation) spectra and emission spectra are characterized by an identical redshift compared to solution. When $\Delta\bar{\nu}_{EC}$ is positive, a redshift of absorption and excitation spectra will be observed if the absolute value of $\Delta\bar{\nu}_s + \Delta_2 - \Delta_1$ is larger than $\Delta\bar{\nu}_{EC}$ or $2\Delta\bar{\nu}_{EC}$ for respectively dimer or larger aggregates while in the opposite case a blueshift will be observed. Due to rapid internal conversion between |+> and |->, the emission will in this case occur from the lowest

excited state |->, and will be shifted by $\Delta\bar{\nu}_{\mathrm{EM,DADS}} = \Delta\bar{\nu}_s + \Delta_2 - \Delta_1 - |\Delta\bar{\nu}_{\mathrm{EC}}|$ or $\Delta\bar{\nu}_{\mathrm{EM,AGGADS}} = \Delta\bar{\nu}_s + \Delta_2 - \Delta_1 - 2|\Delta\bar{\nu}_{\mathrm{EC}}|$ for respectively monomer or large aggregates.[53,54] Hence compared to isolated dye molecules in solution the emission is always redshifted and the Stokes shift is increased by $2\Delta\bar{\nu}_{\mathrm{EC}}$ or $4\Delta\bar{\nu}_{\mathrm{EC}}$ for respectively dimers and large aggregates. This means that even when the absolute value of $\Delta\bar{\nu}_s + \Delta_2 - \Delta_1$ is larger than $\Delta\bar{\nu}_{\mathrm{EC}}$ or $2\Delta\bar{\nu}_{\mathrm{EC}}$, leading to a red shifted absorption, it will still be possible to discriminate between H-type aggregates ($\Delta\bar{\nu}_{\mathrm{EC}} > 0$) and J-type aggregates ($\Delta\bar{\nu}_{\mathrm{EC}} < 0$).

Upon adsorption on the surface of hBN, the excitation spectra of TDC and TD2 do not shift while the emission spectra are redshifted, i.e. the Stokes shift is increased. This suggests the occurrence of H-type aggregation ($\Delta\bar{\nu}_{\mathrm{EC}} > 0$) upon adsorption on hBN. Furthermore, the absence of a shift of the excitation spectra upon adsorption on hBN suggests that the absolute value of $\Delta\bar{\nu}_s + \Delta_2 - \Delta_1$ is close to $\Delta\bar{\nu}_{\mathrm{EC}}$. This agrees with the molecular mechanics simulations (see SI), suggesting H-type packing of the all-*trans* isomer of TDC adsorbed on hBN. In this framework the difference between the shift of the excitation and emission spectra, which amounted to 300 cm^{-1}, corresponds to $2\Delta\bar{\nu}_{\mathrm{EC}}$ (dimers) or to $4\Delta\bar{\nu}_{\mathrm{EC}}$ (large aggregates). This leads to a value of 150 cm^{-1} (dimers) or 75 cm^{-1} (large aggregates) for $\Delta\bar{\nu}_{\mathrm{EC}}$.

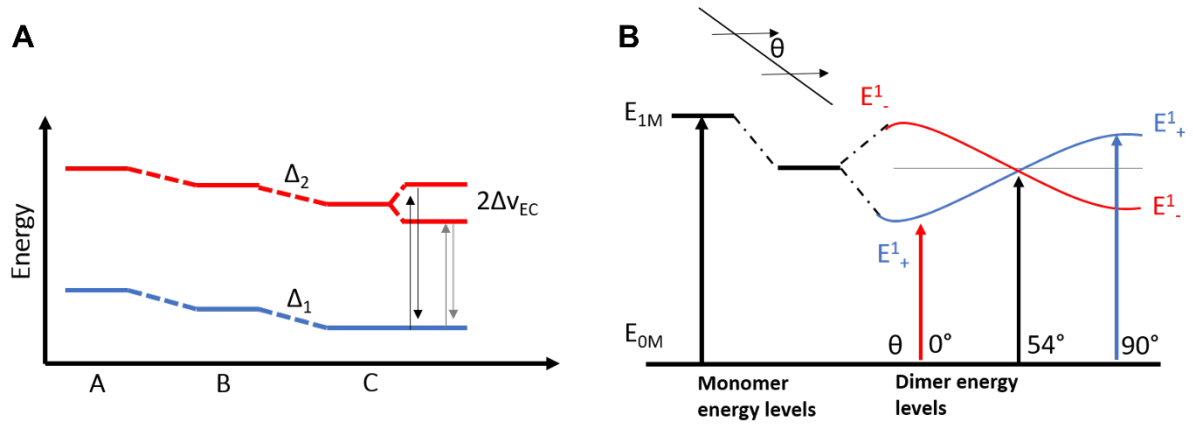

Scheme 1 A Energy scheme of ground (blue) and excited (red) state of A a chromophore in solution, B a chromophore adsorbed on substrate (hBN) and C chromophores aggregating on substrate (left). B Influence of the geometry on the exciton coupling (right).

While it is difficult to estimate Δ_2 - Δ_1, which in absolute value is often smaller than $\Delta\bar{\nu}_{\mathrm{EC}}$, $\Delta\bar{\nu}_{\mathrm{EC}}$ can be estimated knowing the molecular transition dipole, dimensions and packing. $\Delta\bar{\nu}_{\mathrm{EC}}$ can

be approximated by the electrostatic interaction between the transition dipoles.[48–52] While the point dipole approximation of the transition dipoles leads to sometimes a gross overestimation of $\Delta\bar{\nu}_{EC}$, especially when the intermolecular distance becomes small compared to the molecular dimension, Kuhn *et al.* demonstrated that an "extended dipole" approximation leads to value of $\Delta\bar{\nu}_{EC}$, which are very close to those determined by a more sophisticated quantum mechanical approach.[37,55,56] In this approach the point dipole is replaced by two charges $+Q_M$ and $-Q_M$ at a distance L_M, where L_M corresponds to the length of the conjugated system. Q_M and L_M are related to the size of the transition dipole $|\vec{\mu}_M^*|$ by

$$|\vec{\mu}_M^*| = L_M Q_M \qquad \text{Eq. 2}$$

The calculation of the values of $|\vec{\mu}_M^*|$ starting from the absorption spectra in solution is given in the SI (table S7). L_M was determined from the crystallographic data of THIATS[35,57] where it amounts to 2.13 nm. As TDC differs from THIATS only in the structure of the 3- and 3'-substituents this value of L_M can also be used for TDC and THIATS, while it will be about 1.9 nm smaller for TD2 and TD0.

For the packing of the all-*trans* isomer of TDC adsorbed on hBN suggested by molecular mechanics (see SI), $\Delta\bar{\nu}_{EC}$ will now be estimated by the extended dipole approximation. The molecular mechanics suggested a flat-on adsorption where neighboring molecules of TDC are parallel at a distance, R, of about 0.90 nm. Furthermore, the molecules are not shifted relative to one another along their long axis (H-type aggregate). In this case the exciton interaction, $\Delta\bar{\nu}_{EC}$, between two neighboring molecules is given by[55,56]

$$\Delta\bar{\nu}_{EC} = \frac{Q_M^2}{2\pi\varepsilon_0}\left[\frac{1}{R} - \frac{1}{\sqrt{R^2 + L_M^2}}\right] \qquad \text{Eq. 3}$$

With ε_0 the vacuum permittivity (8.85×10^{-12} F m). Using the length of 2.13 nm, a transition dipole of 2.99×10^{-29} C M and an intermolecular separation of 0.91 nm, $\Delta\bar{\nu}_{EC}$ amounts to 0.015 eV or 120 cm^{-1}. This value of 120 cm^{-1} should be considered as upper limit its contribution to

the spectral shift as the calculations assume that the exciton interaction is much larger than the electron-phonon coupling. If this is not the case, exciton interaction between purely electronic states has to be replaced by exciton interaction between vibronic levels, which is reduced by the corresponding Franck-Condon factors, decreasing the respective blue- and redshifts of the $|+\rangle$ state and the $|-\rangle$ state.[48–52] Hence the value of 150 cm^{-1} (dimers) or 75 cm^{-1} (large aggregates) derived from the experimentally observed increase of the Stokes shift for TDC and TD2 is compatible with the packing suggested by the molecular mechanics (see SI) and the adsorption isotherms. This also means that for the excitation (and probably also for the absorption spectrum) the redshift equaling $\Delta\bar{\nu}_S + \Delta_2 - \Delta_1$ is compensated by the blueshift equal to $\Delta\bar{\nu}_{EC}$ or $2\Delta\bar{\nu}_{EC}$. Although such close packing and the resulting exciton interaction would only be expected at a significant coverage of the hBN surfaces by the adsorbed dyes, the corresponding redshift of the emission spectrum is already observed for TDC and TD2 at the lowest coverage (about 2%) where reliable emission spectra could be obtained. This agrees with the AFM data, suggesting that the lowest coverage where AFM micrographs were obtained, the absorbed dye molecules are already clustering (figure S5).

In a similar way, one can try to estimate $\Delta\bar{\nu}_{EC}$ for TD0 starting from the transition dipole derived from the absorption spectrum in solution (2.32×10^{-29} C M, see SI) and the packing suggested by the molecular mechanics calculations. As both packings shown in figure S17 yield a similar packing with flat-on adsorbed molecules shifted parallel to their long axis over respectively 0.41 nm and 0.46 nm and having a nearest neighbor distance along the normal on their long axis of respectively 0.70 nm and 0.77 nm, we will calculate the exciton interaction $\Delta\bar{\nu}_{EC}$ only for the head-to-tail packing, which has the lowest energy.

When it is attempted to estimate for the packing suggested by the molecular mechanics simulations, the exciton interaction, $\Delta\bar{\nu}_{EC}$, between nearest neighbor molecules one has to take into account that the molecules are shifted (head-to-tail packing) by 0.41 nm along their long axis. Therefore, equation 3 has to be replaced by

$$\Delta\bar{\nu}_{EC} = \frac{Q_M^2}{4\pi\varepsilon_0}\left[\frac{2}{\sqrt{R^2 + (0.41x10^{-9})^2}} + \frac{1}{\sqrt{R^2 + \left(L_M - (0.41x10^{-9})\right)^2}}\right.$$

$$\left. + \frac{1}{\sqrt{R^2 + \left(L_M + (0.41x10^{-9})\right)^2}}\right] \qquad \text{Eq. 4}$$

Where R is the distance between neighboring molecules along the normal to their long axis (0.79 nm) and L_M the length of the molecule (1.90 nm). Using equation 2 and 4 a value of 84 cm^{-1} (0.0103 eV) is obtained for $\Delta\bar{\nu}_{EC}$ for the head-to-tail packing. For the alternating head-to-head and tail-to-tail packing, an average value of 82 cm^{-1} (0.010 eV) is obtained for $\Delta\bar{\nu}_{EC}$. The positive values indicate that although neighboring dyes are shifted along their long axis, the exciton interaction still leads to H-type aggregates.

The calculated exciton coupling of TD0 on hBN is only about 50% of that of TDC on hBN. In the framework of the model developed, this explains why the increase of the Stokes shift upon adsorption is 150 cm^{-1} for TD0 versus 300 cm^{-1} for TDC. When $\Delta\bar{\nu}_S + \Delta_2 - \Delta_1$ is similar for TDC and TD0, which is probable when both dyes adsorb flat-on with a similar density, then $\Delta\bar{\nu}_{EM,AGGADS} = \Delta\bar{\nu}_s + \Delta_2 - \Delta_1 - 2|\Delta\bar{\nu}_{EC}|$, which corresponds to the shift of the absorption or excitation spectrum, can be expected to be 150 cm^{-1} smaller (less positive or more negative) for TD0 than for TDC. This explains that while upon adsorption of TDC on hBN nearly no (or a very small) redshift of the excitation spectrum is observed while a significant redshift is observed for TD0.

The AFM micrographs (figure 6A and 6B) indicate clustering of the adsorbed TD0 molecules already at low concentrations of the initial dye solution. This explains why the observed shifts already occur at low concentrations of the initial dye solution.

For THIATS the large redshift of both, the excitation and emission spectrum, lead at most to a minor increase of the Stokes shift upon adsorption on hBN. This is not compatible with the

formation of sandwich type H-aggregates where there is no shift along the long axis of neighboring molecules. When for such aggregates $\Delta\bar{\nu}_{EC}$ is estimated using a length of 2.13 nm, a transition dipole of 2.61x10^{-29} C M (see SI) and an intermolecular separation of 0.45 nm (determined from Q_{sat}) $\Delta\bar{\nu}_{EC}$ amounts to 0.03 eV or 240 cm^{-1}. This is twice the value found for TDC; hence, one should expect an increase of the Stokes shift of 600 cm^{-1} compared to THIATS in solution. As this is not observed, the long axes of neighboring molecules must be shifted significantly leading to very small or even negative values of $\Delta\bar{\nu}_{EC}$, corresponding to J-type rather than H-type aggregation. On the other hand, we do also not observe the typical narrow J-aggregate emission of THIATS at 620 to 640 nm, which is observed in aqueous solution at higher concentrations[27,54], adsorbed to Langmuir layers[17] or in self-assembled films[58]. If typical J-aggregates were formed, one would expect an exciton interaction $\Delta\bar{\nu}_{EC}$ of about 0.09 eV or 700 cm^{-1}, which is much larger than what was calculated above. This indicates that the exciton interaction is much weaker than in typical J-aggregates of THIATS related to a larger intermolecular distance and/or a smaller lateral displacement.

The AFM micrographs indicate clustering of the adsorbed THIATS molecules already at low concentration of the initial dye solution (figure 7A). This explains why the observed shifts already occur at low concentrations of the initial dye solution.

Upon increasing the coverage of the hBN surface, the emission spectra of TDC, TD2 and THIATS and the excitation spectra of TDC and TD2 undergo a further redshift of about 300 cm^{-1}. This could suggest a tighter packing of the adsorbed molecules or an increase of the aggregate size. This will lead to an increase of the absolute value of both Δ_2 - Δ_1 and $\Delta\bar{\nu}_{EC}$ and/or an increase of the effect from the exciton interaction from $\Delta\bar{\nu}_{EC}$ to $2\Delta\bar{\nu}_{EC}$. Increasing the dye concentration in the solution could also induce the formation of multilayers. In the latter case, the second layer of flat-on adsorbed molecules would be at a distance of 0.35 to 0.36 nm from the first layer. Sandwich packing of flat-on adsorbed dyes at this short distance would lead to a significantly larger exciton interaction and hence to a much larger redshift of the emission such as observed for as well J- and H-aggregates of TDC or THIATS in solution.

[27,54,58] In case of H-aggregates it would also lead to a much larger blue shift of the excitation spectra.[53,59] A tighter packing upon increasing the concentration of the initial dye solution is in agreement with the law of mass action.[60] The absence of such shift for TD0 is possibly related to the absence of meso-ethyl moiety, which leads to a more planar structure and hence a stronger interaction of the conjugated system with hBN. This stronger interaction makes the adsorbed layers less sensitive to transition to a closer packing. Such stronger interaction is also reflected in the larger value of K_{LFS} of TD0 compared to TD2, which has a similar conjugated moiety.

4. CONCLUSIONS

In contrast to what generally is observed for the adsorption of cyanine dyes on surfaces or at interfaces, the saturation values of the adsorption isotherms (Q_{Sat}) indicate that the cationic cyanine dyes TDC, TD2 and TD0 adsorb flat-on rather than edge-on on hBN.[17,25,40,41,61] This is confirmed by the excitation and emission spectra of the adsorbed dyes, which do not show the strong exciton interaction expected for the short intermolecular distances for possible edge-on adsorbed dyes. The small exciton interaction also explains why for TDC and TD2 no significant decrease of the FWMH of the excitation and emission spectra typical for the J-aggregates of 9-alkyl substituted cyanine dyes is observed. This tendency for flat-on adsorption reflects the strong interaction between the adsorbed dyes and hBN, which exceeds the π-π interactions between neighboring tightly packed dyes occurring upon edge-on adsorption. In this way adsorption of the cationic cyanine dyes hBN resembles the adsorption of organic molecules to graphite.[62–65] This could also explain the larger value of K_{LFS} observed for TDC, which is substituted by two highly polarizable chlorine atoms. For THIATS, a zwitterionic cyanine dye with an overall negative charge, the value of Q_{Sat} is much too large for flat-on adsorption, but it is still too small for edge-on adsorption suggesting a tilted adsorption. This is again compatible with the excitation and emission spectra, which do not show the features typical for J-aggregates and closely packed edge-on THIATS molecules.[16,18,20,25]

In agreement with the excitation and emission spectra, the AFM experiments indicate that for all dyes investigated aggregation and clustering already occur at low concentrations of the dye solution, which is reflected in a low coverage of hBN by the adsorbed dyes. In analogy to what is observed for the adsorption of organic molecules adsorbed to graphite and porphyrins on hBN.[1] the interaction between neighboring adsorbed molecules is significant. This interaction could be van der Waals interaction between the alkyl-substituents and the pi-system of neighboring molecules in TDC and TD2 (figure S16B) or between interdigitating alkyl-substituents in TD0 (figure S17). Such van der Waals interactions are known to be the driving force for the self-assembly of organic molecules adsorbed to graphite and for governing their packing geometry.[63] Due to the lack of resolution of the AFM experiments and the weak exciton interaction is however not possible to draw any conclusion regarding the long-range order of the adsorbed molecules.

ACKNOWLEDGEMENTS

The authors are thankful for the support from the Research Council of KU Leuven through the project C14/19/079 (FUEPONA), the Research Foundation Flanders (FWO) through the projects G0F8217N and G082215N and a fellowship to J. VdW (11F3520N). R.S. thanks the Department of Chemistry for a fellowship. SFLM acknowledges support from the Austrian Science Fund (FWF, project I3256-N36) and Material Science Institute (Lancaster University) internal funds. The authors want to thank prof. Kenji Watanabe and prof. Takashi Taniguchi of the NIMS (National Institute of Material Science) institute of Japan for a gift of the hBN crystals.

REFERENCES

1. Korolkov VV, Svatek SA, Summerfield A, et al. van der Waals-Induced Chromatic Shifts in Hydrogen-Bonded Two-Dimensional Porphyrin Arrays on Boron Nitride. *ACS Nano*. 2015;9(10):10347-10355. doi:10.1021/acsnano.5b04443

2. Weng Q, Wang X, Wang X, Bando Y, Golberg D. Functionalized hexagonal boron nitride nanomaterials: emerging properties and applications. *Chem. Soc. Rev*. 2016;45(14):3989-4012. doi:10.1039/C5CS00869G

3. Jiang XF, Weng Q, Wang XB, et al. Recent Progress on Fabrications and Applications of Boron Nitride Nanomaterials: A Review. *J. Mater. Sci. Technol*.

2015;31(6):589-598. doi:10.1016/j.jmst.2014.12.008

4. Lin Y, Connell JW. Advances in 2D boron nitride nanostructures: nanosheets, nanoribbons, nanomeshes, and hybrids with graphene. *Nanoscale*. 2012;4(22):6908. doi:10.1039/c2nr32201c

5. Shi Y, Hamsen C, Jia X, et al. Synthesis of Few-Layer Hexagonal Boron Nitride Thin Film by Chemical Vapor Deposition. *Nano Lett*. 2010;10(10):4134-4139. doi:10.1021/nl1023707

6. Cai Q, Scullion D, Gan W, et al. High thermal conductivity of high-quality monolayer boron nitride and its thermal expansion. *Sci. Adv*. 2019;5(6):eaav0129. doi:10.1126/sciadv.aav0129

7. Cho YJ, Summerfield A, Davies A, et al. Hexagonal Boron Nitride Tunnel Barriers Grown on Graphite by High Temperature Molecular Beam Epitaxy. *Sci. Rep*. 2016;6(1):34474. doi:10.1038/srep34474

8. Ahmed R, Fazal-e-Aleem, Hashemifar SJ, Akbarzadeh H. First principles study of structural and electronic properties of different phases of boron nitride. *Phys. B Condens. Matter*. 2007;400(1-2):297-306. doi:10.1016/j.physb.2007.08.012

9. Kim DH, Kim HS, Song MW, Lee S, Lee SY. Geometric and electronic structures of monolayer hexagonal boron nitride with multi-vacancy. *Nano Converg*. 2017;4(1):13. doi:10.1186/s40580-017-0107-0

10. Arnold T, Forster M, Fragkoulis AA, Parker JE. Structure of Normal-Alkanes Adsorbed on Hexagonal-Boron Nitride. *J. Phys. Chem. C*. 2014;118(5):2418-2428. doi:10.1021/jp4063059

11. Albar JD, Korolkov VV, Baldoni M, et al. Adsorption of Hexacontane on Hexagonal Boron Nitride. *J. Phys. Chem. C*. 2018;122(1):27575-27581. doi:10.1021/acs.jpcc.8b10167

12. Kerfoot J, Svatek SA, Korolkov VV, et al. Fluorescence and Electroluminescence of J-Aggregated Polythiophene Monolayers on Hexagonal Boron Nitride. *ACS Nano*. 2020;14(10):13886-13893. doi:10.1021/acsnano.0c06280

13. Mertens SFL, Hemmi A, Muff S, et al. Switching stiction and adhesion of a liquid on a solid. *Nature*. 2016;534(7609):676-679. doi:10.1038/nature18275

14. Mertens SFL. Copper underpotential deposition on boron nitride nanomesh. *Electrochim. Acta*. 2017;246:730-736. doi:10.1016/j.electacta.2017.06.082

15. Kerfoot J, Korolkov VV, Nizovtsev AS, et al. Substrate-induced shifts and screening in the fluorescence spectra of supramolecular adsorbed organic monolayers. *J. Chem. Phys*. 2018;149(5):054701. doi:10.1063/1.5041418

16. Rousseau E, Koetse MM, Van der Auweraer M, De Schryver FC. Comparison between J-aggregates in a self-assembled multilayer and polymer-bound J-aggregates in solution: a steady-state and time-resolved spectroscopic study. *Photochem. Photobiol. Sci*. 2002;1(6):395-406. doi:10.1039/b201690g

17. Vranken N, Van der Auweraer M, De Schryver FC, Lavoie H, Bélanger P, Salesse C. Influence of Molecular Structure on the Aggregating Properties of Thiacarbocyanine Dyes Adsorbed to Langmuir Films at the Air−Water Interface. *Langmuir*. 2000;16(24):9518-9526. doi:10.1021/la000896l

18. Vranken N, Jordens S, De Belder G, et al. The Influence of Meso-Substitution on the Photophysical Behavior of Some Thiacarbocyanine Dyes in Dilute Solution. *J. Phys.*

Chem. A. 2001;105(45):10196-10203. doi:10.1021/jp0123536

19. Noukakis D, Van de Auweraer M, Toppet S, De Schryver FC. Photophysics of thiacarbocyanine dye in organic solvent. *J. Phys. Chem*. 1995;99(31):11860-11866. doi:10.1021/j100031a012

20. Khimenko V, Chibisov AK, Görner H. Effects of Alkyl Substituents in the Polymethine Chain on the Photoprocesses in Thiacarbocyanine Dyes. *J. Phys. Chem. A*. 1997;101(39):7304-7310. doi:10.1021/jp971472b

21. Van der Auweraer M, Van den Zegel M, Boens N, De Schryver FC, Willig F. Photophysics of 2-phenyl-3-indolocarbocyanine dyes. *J. Phys. Chem*. 1986;90(6):1169-1175. doi:10.1021/j100278a041

22. Pevenage D, Corens D, Dehaen W, Van der Auweraer M, De Schryver FC. Influence of the N-Substituent on the Photophysical Properties of Oxacarbocyanines in Solution. *ChemInform*. 2010;29(12). doi:10.1002/chin.199812153

23. Haverkort F, Stradomska A, Knoester J. First-Principles Simulations of the Initial Phase of Self-Aggregation of a Cyanine Dye: Structure and Optical Spectra. *J. Phys. Chem. B*. 2014;118(29):8877-8890. doi:10.1021/jp5049277

24. Khairutdinov RF, Serpone N. Photophysics of Cyanine Dyes: Subnanosecond Relaxation Dynamics in Monomers, Dimers, and H- and J-Aggregates in Solution. *J. Phys. Chem. B*. 1997;101(14):2602-2610. doi:10.1021/jp9621134

25. Vranken N, Foubert P, Köhn F, et al. Influence of the Deposition Method on the Topography and Spectroscopy of J-Aggregates of a Thiacarbocyanine Dye Adsorbed to a Langmuir Film. *Langmuir*. 2002;18(22):8407-8417. doi:10.1021/la020230m

26. Drobizhev MA, Sapozhnikov MN, Scheblykin IG, Varnavsky OP, Van der Auweraer M, Vitukhnovsky AG. Exciton dynamics and trapping in J-aggregates of carbocyanine dyes. *Pure Appl. Opt.* 1996;5(5):569-581. doi:10.1088/0963-9659/5/5/011

27. Drobizhev MA, Sapozhnikov MN, Scheblykin IG, Varnavsky OP, Van der Auweraer M, Vitukhnovsky AG. Relaxation and trapping of excitons in J-aggregates of a thiacarbocynine dye. *Chem. Phys*. 1996;211(1-3):455-468. doi:10.1016/0301-0104(96)00134-6

28. Haverkort F, Stradomska A, de Vries AH, Knoester J. Investigating the Structure of Aggregates of an Amphiphilic Cyanine Dye with Molecular Dynamics Simulations. *J. Phys. Chem. B*. 2013;117(19):5857-5867. doi:10.1021/jp4005696

29. Steeno R, Rodríguez González MC, Eyley S, Thielemans W, Mali KS, De Feyter S. Covalent Functionalization of Carbon Surfaces: Diaryliodonium versus Aryldiazonium Chemistry. *Chem. Mater*. 2020;32(12):5246-5255. doi:10.1021/acs.chemmater.0c01393

30. Polak E, Ribiere G. Note sur la convergence de méthodes de directions conjuguées. *ESAIM Math Model Numer Anal - Modélisation Mathématique Anal Numérique*. 1969;3:35-43. http://www.numdam.org/item/M2AN_1969__3_1_35_0/

31. Vandenwijngaerden JBF. Self-assembly of dyes on boron nitride substrata: a spectroscopic and morphological characterisation. KU Leuven. Faculteit Wetenschappen. 2019

32. Atkins P, de Paula J. *Atkins' Physical Chemistry*. 10th ed. Oxford University Press; 2014.

33. Ambroz F, Macdonald TJ, Martis V, Parkin IP. Evaluation of the BET Theory for the

Characterization of Meso and Microporous MOFs. *Small Methods*. 2018;2(11):1800173. doi:10.1002/smtd.201800173

34. Jeppu GP, Clement TP. A modified Langmuir-Freundlich isotherm model for simulating pH-dependent adsorption effects. *J. Contam. Hydrol*. 2012;129-130:46-53. doi:10.1016/j.jconhyd.2011.12.001

35. Van der Auweraer M, Scheblykin I. One-dimensional J-aggregates: Dependence of the properties of the exciton band on the model of the intermolecular coupling. *Chem. Phys*. 2002;275(1-3):285-306. doi:10.1016/S0301-0104(01)00528-6

36. Würthner F, Kaiser TE, Saha-Möller CR. J-Aggregates: From Serendipitous Discovery to Supramolecular Engineering of Functional Dye Materials. *Angew. Chem. Int. Ed*. 2011;50(15):3376-3410. doi:10.1002/anie.201002307

37. Kuhn H, Kuhn C. CHROMOPHORE COUPLING EFFECTS. In: *J-Aggregates*. World Scientific; 1996:1-40. doi:10.1142/9789812830029_0001

38. Tian CH, Zoriniants G, Gronheid R, Van der Auweraer M, De Schryver FC. Confocal Fluorescence Microscopy and AFM of Thiacyanine J Aggregates in Langmuir-Schaefer Monolayers. *Langmuir*. 2003;19(23):9831-9840. doi:10.1021/la034817s

39. Gretchikhine A, Schweitzer G, Van der Auweraer M, De Keyzer R, Vandenbroucke D, De Schryver FC. Femtosecond transient absorption and luminescence decay studies of spectrally sensitized photographic emulsions. *J. Appl. Phys*. 1999;85(3):1283-1293. doi:10.1063/1.369259

40. Karthaus O, Kawatani Y. Self-Assembly and Aggregation Control of Cyanine Dyes by Adsorption onto Mesoscopic Mica Flakes. *Jpn J. Appl. Phys*. 2003;42:127-131. doi:10.1143/JJAP.42.127

41. Yao H, Sugiyama S, Kawabata R, et al. Spectroscopic and AFM Studies on the Structures of Pseudoisocyanine J Aggregates at a Mica/Water Interface. *J. Phys. Chem. B*. 1999;103(21):4452-4456. doi:10.1021/jp990127e

42. Mertens SFL. Adsorption and Self-Organization of Organic Molecules under Electrochemical Control. In: Wandelt K, ed. *Encyclopedia of Interfacial Chemistry*. Elsevier; 2018:13-23. doi:10.1016/B978-0-12-409547-2.13061-6

43. Cui K, Dorner I, Mertens SFL. Interfacial supramolecular electrochemistry. *Curr. Opin. Electrochem*. 2018;8:156-163. doi:10.1016/j.coelec.2018.06.002

44. Brooker LGS, White FL, Heseltin DW, Keyes GH, Dent SG, Van Lare EJ. Spatial Configuration, Light Absorption, and Sensitizing Effects of Cyanine Dyes. *J. Photogr. Sci*. 1953;1(6):173-183. doi:10.1080/03700240.1953.11736602

45. Caldwell JD, Aharonovich I, Cassabois G, Edgar JH, Gil B, Basov DN. Photonics with hexagonal boron nitride. *Nat. Rev. Mater*. 2019;4(8):552-567. doi:10.1038/s41578-019-0124-1

46. Qin W, Rohand T, Baruah M, et al. Solvent-dependent photophysical properties of borondipyrromethene dyes in solution. *Chem. Phys. Lett*. 2006;420(4-6):562-568. doi:10.1016/j.cplett.2005.12.098

47. Qin W, Baruah M, Van der Auweraer M, De Schryver FC, Boens N. Photophysical Properties of Borondipyrromethene Analogues in Solution. *J. Phys. Chem. A*. 2005;109(33):7371-7384. doi:10.1021/jp052626n

48. Kasha M. Energy Transfer Mechanisms and the Molecular Exciton Model for Molecular Aggregates. *Radiat. Res*. 1963;20(1). doi:10.2307/3571331

49. Kasha M. Relation between Exciton Bands and Conduction Bands in Molecular Lamellar Systems. *Rev. Mod. Phys*. 1959;31(1):162-169.

50. McRae EG, Kasha M. The Molecular Exciton Model. In: *Physical Processes in Radiation Biology*. Elsevier; 1964:23-42. doi:10.1016/B978-1-4831-9824-8.50007-4

51. Davydov AS. The Theory of Molecular Excitons. *Sov. Phys. Usp*. 1964;82(3):393-448. doi:10.3367/UFNr.0082.196403a.0393

52. Förster T. Delocalization excitation and excitation transfer. In: *Modern Quantum Chemistry*. Vol 3. Academic Press; 1965:93-137.

53. Van Der Auweraer M, Biesmans G, De Schryver FC. On the photophysical properties of aggregates of 3-(2-phenyl)-indolocarbocyanines. *Chem. Phys*. 1988;119(2-3):355-375. doi:10.1016/0301-0104(88)87196-9

54. Scheblykin I, Varnavsky O, Verbouwe W, De Backer S, Van der Auweraer M, Vitukhnovsky A. Relaxation dynamics of excitons in J-aggregates revealing a two-component Davydov splitting. *Chem. Phys. Lett*. 1998;282(3-4):250-256. doi:10.1016/S0009-2614(97)01290-6

55. Czikklely V, Forsterling HD, Kuhn H. Extended dipole model for aggregates of dye molecules. *Chem. Phys. Lett*. 1970;6(3):207-210. doi:10.1016/0009-2614(70)80220-2

56. Czikkely V, Försterling HD, Kuhn H. Light absorption and structure of aggregates of dye molecules. *Chem. Phys. Lett*. 1970;6(1):11-14. doi:10.1016/0009-2614(70)80062-8

57. Asanuma H, Ogawa K, Fukunaga H, Tani T, Tanaka J. In: *Internation Congress on Imaging Science*. ICPS; 1998:178.

58. Rousseau E, Van Der Auweraer M, De Schryver FC. Steady-state and time-resolved spectroscopy of a self-assembled cyanine dye multilayer. *Langmuir*. 2000;16(23):8865-8870. doi:https://doi.org/10.1021/la000247+

59. Biesmans G, Van der Auweraer M, De Schryver FC. Influence of deposition circumstances on the spectroscopic properties of mixed monolayers of dioctadecyloxacarbocyanine and arachidic acid. *Langmuir*. 1990;6(1):277-285. doi:10.1021/la00091a045

60. Lei S, Tahara K, De Schryver FC, Van der Auweraer M, Tobe Y, De Feyter S. One Building Block, Two Different Supramolecular Surface-Confined Patterns: Concentration in Control at the Solid–Liquid Interface. *Angew. Chem. Int. Ed*. 2008;47(16):2964-2968. doi:10.1002/anie.200705322

61. Jeunieau L, Verbouwe W, Rousseau E, Van der Auweraer M, Nagy JB. Interaction of an Oxa- and Thiacarbocyanine Dye and Silver Halide Nanoparticles Synthesized in a Microemulsion System. *Langmuir*. 2000;16(4):1602-1611. doi:10.1021/la9906368

62. De Feyter S, Gesquière A, Abdel-Mottaleb MM, et al. Scanning Tunneling Microscopy: A Unique Tool in the Study of Chirality, Dynamics, and Reactivity in Physisorbed Organic Monolayers. *Acc. Chem. Res*. 2000;33(8):520-531. doi:10.1021/ar970040g

63. Velpula G, Martin C, Daelemans B, et al. “Concentration-in-Control” self-assembly concept at the liquid–solid interface challenged. *Chem. Sci*. 2021;12(39):13167-13176. doi:10.1039/D1SC02950A

64. Verstraete L, Rinkovec T, Cao H, Reeves HI, Harvey JN, De Feyter S. Chiral Adsorption Conformations of Long-Chain n -Alkanes Induced by Lattice Mismatch. *J.*

Phys. Chem. C. 2021;125(2):1557-1563. doi:10.1021/acs.jpcc.0c09825

65. González-Rodríguez D, Janssen PGA, Martín-Rapún R, et al. Persistent, Well-Defined, Monodisperse, π-Conjugated Organic Nanoparticles via G-Quadruplex Self-Assembly. *J. Am. Chem. Soc*. 2010;132(13):4710-4719. doi:10.1021/ja908537k